Theor Chim Acta (1990) 77: 39–56

Theoretica Chimica Acta

Semiempirical study of electronic and bonding properties of iron silicide clusters

Leonardo J. Rodríguez[1], Fernando Ruette[2], Germán R. Castro[3], Eduardo V. Ludeña[2], and Antonio J. Hernández[4]

[1] Departamento de Química, Universidad del Zulia, Maracaibo, Venezuela
[2] Laboratorio de Físico Química Teórica, Centro de Química, Instituto Venezolano de Investigaciones Científicas, Apdo. 21827, Caracas 1020-A, Venezuela
[3] Departamento de Física, Universidad Central de Venezuela, Apdo. 2120, Caracas, Venezuela
[4] Departamento de Química, Universidad Simón Bolívar, Apdo. 89000, Caracas, 1080-A, Venezuela

(Received May 15, 1989; received in revised form August 9/Accepted August 14, 1989)

Summary. Molecular orbital calculations of iron, silicon, and iron silicide clusters have been carried out using the UHF-MINDO/SR method. The nature of the bonding in these compounds has been investigated by analyzing the importance of bonding indexes and diatomic components of the total energy. It has been found that in iron silicide the strongest bond is formed between Fe–Si and that it arises mainly as the result of *sp-sp* type orbital interactions. Although *d* orbitals show very little overlap with *s-p* orbitals, they do contribute significantly to bonding through electrostatic type diatomic interactions. By means of a detailed analysis of *sp*, and *d* orbitals and total density of states (DOS) of Fe_7Si_7, Si_7Fe_7, Fe_{15}, and Si_{17} clusters, the present calculations have permitted us to explain the origin of the iron silicide UPS experimental peaks.

Key words: MINDO/SR — Clusters — Iron silicide — Density of states — Bonding properties

1. Introduction

Because of the technological importance of transition metal silicides in metal/Si contacts in electronic devices, as well as their own magnetic and metallurgic properties, these compounds have been receiving increased attention in the last few years. Among the metal silicides, FeSi has been the object of several experimental studies due to its special properties. A variety of surface spectroscopy techniques such as X-ray photoelectron spectroscopy (XPS) [1, 4], bremsstrahlung isochromat spectroscopy (BIS) [4], inelastic neutron scattering (INS) [5], ultraviolet photoelectron spectroscopy (UPS) [1, 6], Auger-electron

spectroscopy (AES) [1, 7], electron-energy-loss spectroscopy (EELS) [1, 7a], magnetic susceptibility [8], electrical conductivity [9], etc. have been applied to FeSi in order to elucidate its electronic structure and to determine how the latter correlates with its physical and chemical properties.

In spite of this experimental effort, the understanding of the FeSi electronic structure is still unclear. In addition, the lack of theoretical studies on iron-silicides, except for a previous communication [10], justifies the present application of the MINDO/SR method [11] to this bimetallic system.

In the next section, a brief review of the methodology used in these calculations is presented. An analysis of the FeSi diatomic molecule is carried out in Sect. 3.1. The calculated binding properties and density of states of Fe_7Si_7, Si_7Fe_7, Fe_{15} and Si_{17} clusters are discussed in Sects. 3.2, 3.3 and 3.4 and are compared with recent experimental work. Particular emphasis is placed on understanding the nature of the FeSi bond and in elucidating the role of *d* orbitals in the formation of these compounds.

2. Theoretical background

The UHF-MINDO/SR method [11] is an extension of MINDO/3 [12] that permits the treatment of transition metals and the inclusion of selective molecular orbital occupancies and symmetries [13]. In previous publications [14–19], it has been shown that the MINDO/SR method leads to a very reasonable description of the electronic and bonding properties of catalytic systems that contain transition metals, surface as well as bulk properties of metal clusters, and of adsorbent-adsorbate interactions in chemisorption processes. Needless to say, the success of this method is largely dependent upon the procedure used in estimating the ground state molecular parameters. The Fe atomic and bonding Fe–Fe parameters used in this paper were reported in a previous work dealing with the electronic structure of iron clusters [14]. For silicon, we have adopted the parameters described by Bingham, Dewar and Lo [12] as they give a good correlation between the equilibrium bond properties of Si_2, with the experimental bond length of 2.25 Å, and the experimental dissociation energy of 75 kcal/mol [20]. In addition, the quality of these parameters has been tested successfully by several calculations [21] on clusters that contain silicon atoms. The FeSi diatomic molecule has not been reported either theoretically or experimentally, and therefore an extensive search for bonding parameters was not attempted in this work. Our choice of the FeSi bond length was based on an extrapolation based on the bond lengths in Fe_2 and Si_2 diatomic molecules and the correspondent equilibrium internuclear distances in Fe and Si bulks. This relationship was applied to the FeSi bulk taking into account an average value for the nearest Fe–Si distances. The value of 2.25 Å thus obtained is a judicious selection in view of the fact that it is just a bit shorter than the bulk FeSi distance which is 2.29 Å. Our parameters were selected so as to reproduce this distance and also the atomization energy of 70.0 kcal/mol [22] which is the only known experimental fact about this system. The conjecture that our calculated ground state for the

FeSi molecule is a reasonable one is based on the observation that a 20% variation of the parameters did not change the symmetry or the orbital occupation numbers of this ground state. Furthermore, the bond polarity is in agreement with that estimated from atomic electronegativity considerations. A summary of the parameters used in these calculations is presented in Table 1.

The theoretical tool of density of states (DOS) has been used to evaluate the electronic properties of *sp* and *d* bands. A Gaussian approximation described by Simonetta and Gavezzotti [23] permits us to construct the DOS from the calculated ionization energies obtained using Koopmans' theorem. The DOS was calculated separately for the total, *sp*, and *d* orbitals of all clusters studied.

In order to analyze the nature and strength of cluster bonds the well-known energy partitioning technique [24, 25], first employed in the context of the CNDO and INDO methods, was utilized for the present MINDO/SR calculations [17]. In this approach, the total energy expression for a molecule is written

Table 1. Atomic and molecular parameters (eV)

Slater exponent and core parameters

Atom	Atomic orbital	Slater exponent $(a.u.)^{-1}$	Core parameters
	4*s*	1.36	−102.13
Fe	4*p*	1.20	− 74.57
	3*d*	3.73	−127.29
Si	3*s*	1.63	− 39.82
	3*p*	1.38	− 29.15

Slater–Condon parameters

Fe	3*d*-3*d*	3*d*-4*s*	3*d*-4*p*	4*s*-4*s*	4*s*-4*p*	4*p*-4*p*
F^0	17.86426	13.74957	10.07612	13.84500	9.48361	8.28022
F^2	8.41423	—	0.67693	—	2.45289	—
F^4	5.10633	—	—	—	—	—
G^1	—	—	0.25098	—	2.20164	—
G^2	—	1.38466	—	—	—	—
G^3	—	—	0.16581	—	—	—

Si	2*s*-2*s*	2*s*-2*p*	2*p*-2*p*
F^0	0.36089	0.30723	0.24978
F^2	0.11791	—	—
G^1	0.14553	—	—

Molecular parameters

Diatomic molecule	α	β
Fe–Fe	1.01000	0.60300
Si–Si	0.91842	0.24170
Fe–Si	3.00175	0.67739

as a sum $\sum_x E_X$ of one center energy terms (E_x is the energy associated with the atom X) plus a sum $\sum_{x \neq y} E_{XY}$ (E_{XY} corresponds to the interaction energy between atoms X and Y). The two-center terms E_{XY} (diatomic contributions to the total energy) are further partitioned into the potential energy of electrons X in the field of nucleus Y and vice versa, the electronic repulsion energy between electrons on atoms X and Y, the contribution of the resonance integrals to the energy of the X–Y bond, the electronic exchange interactions of the electrons on atoms X and Y, and the nuclear repulsion energy between nuclei X and Y. We have calculated each one of the above energies for the *s-s*, *p-p*, *d-d*, *s-p*, *s-d* and *p-d* orbital interactions with the purpose of analyzing their relative importance in the bonds of the compounds studied in the present work.

3. Iron-silicon interactions

3.1. Bonding in diatomic FeSi

According to our calculations the ground state of FeSi corresponds to a triplet state ($^3\Delta$) with four electrons entirely localized on the iron atom, and with holes in $\delta(d)$ and $3\sigma^*$ orbitals.

The calculated bonding properties and their experimental values (in parentheses) for the ground states of Fe_2, Si_2 and FeSi are presented in Table 2. From an examination of the orbital occupancies shown in Table 2, one sees that the atomic electronic configurations in Fe_2, Si_2, and FeSi are Fe($s^{0.76}$, $p^{0.24}$, $d^{7.00}$), Si($s^{1.83}$, $p^{2.17}$), and Fe($s^{1.09}$, $p^{0.78}$, $d^{6.01}$) and Si($s^{1.54}$, $p^{2.58}$), respectively. The comparison of these values indicates that the Fe–Si interaction gives rise to a charge redistribution. Table 2 also shows a Si(*sp*)–Fe(*d*) Mulliken bond order of zero, which eliminates the possibility of a direct bonding between the Fe($3d_{z^2}$) and the *sp* atomic orbitals of silicon. This nonbonding feature of the Fe(3*d*) orbitals has also been found in connection with electron spectroscopy studies of iron silicide [4, 6]. The magnitude of the FeSi interactions is indicated by the value of 2.04 for the Si(*sp*)–Fe(*sp*) Mulliken bond order shown in Table 2 and the net electron density transfer of 0.12 from Fe to Si (see orbital occupancies in Table 2); this fact, of course is in agreement with the more electronegative character of Si as compared with the Fe atom in diatomic FeSi.

Figure 1 depicts the molecular orbital diagram calculated for the ground state of FeSi. The main covalent σ bonding interaction is represented in this figure by the $2\sigma(\alpha)$ molecular level, which is about 50% localized on the Fe and the Si atoms, respectively, and is mainly formed from the interaction of a Fe($4s$, $4p$, $3d_{z^2}$) hybrid orbital and the $3s$ atomic orbital of silicon. The indirect contribution of the $3d_{z^2}$ orbital to the bonding will be explained in more detail below in Sect. 3.3. Its population in the free iron atom is $2e^-$ whereas in FeSi it is $1e^-$. This result indicates that the iron hybridization represents the main mechanism for a nonbonding transfer of electronic density away from the Fe(3*d*) into the Fe(4*p*) orbital, i.e., for the change from an isolated Fe($4s^1$, $3d^7$) configuration into the Fe($4s^{1.1}$, $4p^{0.8}$, $3d^6$) electronic configuration found in

Table 2. Calculated properties of Fe_2, Si_2 and FeSi

Molecule	Orbital occupancies			Mulliken bond order		Bond length (Å)	Binding energy (kcal/mol)
	s	*p*	*d*	*sp-sp*	*sp-d*		
$Fe_2(^7\Delta)$[a]	0.76	0.24	7.00	1.83	0.01	2.35 (2.40)[a]	-15.3 (-18 ± 4)[a]
$Si_2(^3\Sigma_g)$[b]	1.83	2.17	—	1.38	—	2.25 (2.246)[b]	-76.1 (-74 ± 3)[c]
FeSi($^3\Delta$) Fe	1.09	0.78	6.01	2.04	0.00	2.25	-69.8 (-70 ± 6)[c]
Si	1.54	2.58	—				

[a] From [29a]
[b] From [20]
[c] From [22]

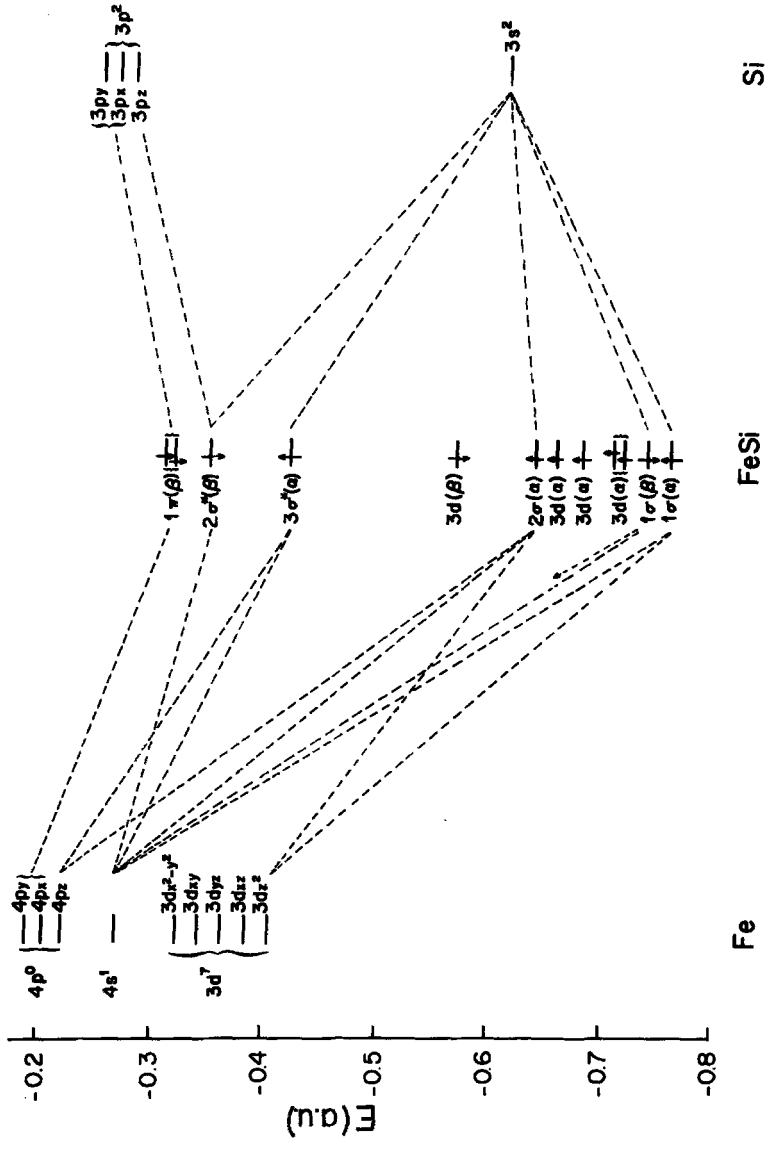

Fig. 1. Molecular orbitals diagram for diatomic FeSi

diatomic FeSi. A different behavior is observed in the other σ and π molecular orbitals. The $3\sigma^*(\alpha)$ and $1\sigma(\alpha)$ levels are 80% and 90% localized on Fe, respectively. On the other hand, the $3\sigma^*(\beta)$ and $1\sigma(\beta)$ are 90% and 80% confined to the silicon atom, respectively. The $1\pi(\beta)$ molecular orbitals are formed by the interaction Fe($4p$)–Si($3p$) atomic orbitals and are 83% centered on the silicon atom.

An analysis of Mulliken bond orders is given, taking into account individual contributions coming from each molecular orbital. The results show that the molecular orbitals that contribute the most to the bond are $1\sigma(\alpha)$ (0.106), $2\sigma(\alpha)$ (0.615), $1\sigma(\beta)$ (0.614), $2\sigma(\beta)$ (0.187) and $2\pi(\beta)$ (0.478). In accord with these results we can conclude that the Fe–Si bond is mostly formed by σ type orbitals with some contribution from π orbitals. Some degree of ionic character is observed due to the charge transfer and the localization of several σ and π orbitals on the Fe or Si atoms.

3.2. Iron-silicide clusters

The bulk crystal structure [26] of iron silicide is a B-20 cubic with Fe atoms in $(X, X, X; X + 1/2, 1/2 - X, -X;)$ positions and four Si atoms in equivalent ones. The unit cell constants are: $a = 4.489$ Å, $X_{Fe} = 0.137$ and $X_{Si} = 0.842$ [27]. In this cell each Fe atom is bonded to seven Si atoms in the first coordination sphere and to six Fe atoms in the second one. The Fe atoms are surrounded by one Si atom at 2.29 Å (A distance), three at 2.34 Å (B distances), and three at 2.52 Å (C distances). The second coordination sphere is formed by six Fe atoms at 2.75 Å (D distances). The Si atoms present similar coordination spheres: a first one with seven iron atoms at the Fe–Si distances cited above and a second one with six Si atoms at 2.78 Å (E distances).

Based on these structural characteristics, and on the criterion that at least one atom must have a complete coordination environment, 14-atom clusters having complete first and second coordination spheres were chosen to represent the FeSi bulk. This is depicted in Fig. 2, where the central atom can be taken either as iron (Fe_7Si_7) or as silicon (Si_7Fe_7). In this way our bulk model has a well represented central atom. In order to assess the relative magnitude of the Si–Si and Fe–Fe interactions in the FeSi clusters studied in this paper, iron and silicon clusters which model bulk iron and bulk silicon, were also constructed for comparison. The iron cluster consisting of 15 Fe atoms with a body centered cubic crystallographic structure is also shown in Fig. 3a (in which the central atom is completely coordinated). The Si cluster with diamond structure formed from 17 Si atoms is depicted in Fig. 3b, where the central atom is bonded to first and second nearest neighbors.

An examination of the most stable multiplicities for each of the clusters described above was carried out. The optimal values of 23, 19, 47 and 1 were found for Fe_7Si_7, Si_7Fe_7, Fe_{15} and Si_{17} clusters, respectively. The number of unpaired electrons per each iron atom corresponds to 3.14 and 2.57 for the Fe_7Si_7 and Si_7Fe_7 clusters, respectively. These values are close to the value of

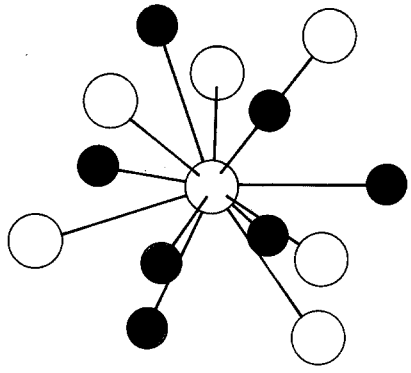

Fig. 2. Iron silicide cluster (Fe_7Si_7 or Si_7Fe_7). ○, Si; ●, Fe in Fe_7Si_7 and ○, Fe; ●, Si in Si_7Fe_7

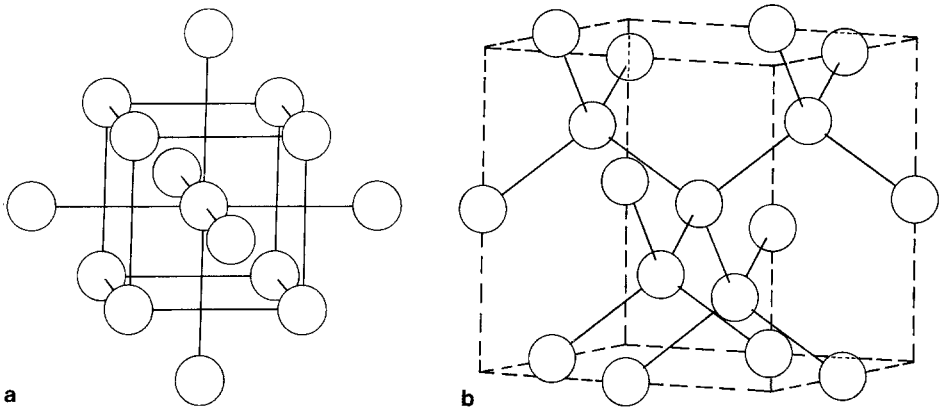

Fig. 3. **a** Iron cluster (Fe_{15}); **b** Silicon cluster (Si_{17})

3.06 found for Fe_{15} confirming the fact that iron silicide is in a paramagnetic state [5, 6].

3.3. Bonding properties

The bonding properties and the electronic populations of FeSi (diatomic molecule) and of all the clusters studied in this work are presented in Table 3. For the analysis of bonding properties of these systems, we have relied on the Mulliken bond orders (MBO) and on the components of the total energy, the so-called "diatomic energies" (DE) [17, 24, 25]. For the sake of simplicity the values of all properties of the Fe–Fe, Fe–Si and Si–Si bonds shown in Table 3 were taken to be the average values for different bond lengths where only two types of bonds were considered, namely, those involving the central atom and those including two peripheral atoms. In the case of the Fe_{15} cluster, two interatomic distances were considered. They were labeled as *F* (Fe–Fe distance of 2.48 Å) and *G* (Fe–Fe distance of 2.87 Å). For the Si_{17} cluster, we also have

Table 3. Bond orders diatomic energies, and orbital populations of Fe_7Si_7, Si_7Fe_7, Fe_{15} and Si_{17} clusters

Cluster	Bond Y–X	Mulliken Bond orders			Diatomic energies (a.u.)	Valence orbital population on Atom X(e^-)		
		sp-sp	*sp-d*	Total		*sp*	*d*	Total
Fe_7Si_7	Fe^a–Si(*A*)	0.92	0.01	0.93	−0.132	3.63	—	3.63
	Fe^a–Si(*B*)	0.95	0.01	0.96	−0.176	3.41	—	3.41
	Fe^a–Si(*C*)	0.67	0.00	0.67	−0.130	3.54	—	3.54
	Fe^a–Fe(*D*)	0.44	0.00	0.45	−0.041	1.42	6.99	8.41
	——Fe^a	—	—	—	—	1.58	6.99	8.57
	Si–Fe(*A*)	1.52	0.01	1.53	−0.340	1.44	6.99	8.43
	Si–Fe(*B*)	1.40	0.00	1.40	−0.321	1.56	6.99	8.55
	Si–Fe(*C*)	1.31	0.00	1.31	−0.303	1.65	6.99	8.64
	Fe–Fe(*D*)	0.75	0.01	0.76	−0.037	1.44	6.99	8.43
Si_7Fe_7	Si^a–Fe(*A*)	0.92	0.00	0.92	−0.243	1.66	6.99	8.65
	Si^a–Fe(*B*)	0.95	0.00	0.95	−0.212	1.44	6.99	8.43
	Si^a–Fe(*C*)	0.67	0.00	0.67	−0.211	1.65	6.99	8.64
	Si^a–Si(*E*)	0.31	—	0.31	−0.024	3.64	—	3.64
	——Si^a	—	—	—	—	2.74	—	2.74
	Fe–Si(*A*)	1.50	—	1.50	−0.340	3.48	—	3.48
	Fe–Si(*B*)	1.49	—	1.49	−0.375	3.64	—	3.64
	Fe–Si(*C*)	1.31	—	1.31	−0.301	3.64	—	3.64
	Si–Si(*E*)	0.62	—	0.62	−0.019	3.64	—	3.64
Fe_{15}	Fe–Fe^a(*F*)	0.77	0.00	0.77	−0.081	0.96	6.99	7.95
	Fe^a–Fe(*G*)	0.62	0.00	0.62	−0.067	1.03	6.99	8.02
	Fe–Fe(*F*)	0.93	0.00	0.93	−0.113	0.99	6.99	7.98
Si_{17}	Si–Si^a(*H*)	1.26	—	1.26	−0.377	3.68	—	3.68
	Si^a–Si(*I*)	0.22	—	0.22	−0.003	3.92	—	3.92
	Si–Si(*H*)	1.42	—	1.42	−0.395	4.32	—	4.32
FeSi	Fe–Si	2.04	0.000	2.04	−0.522	4.12	—	4.12

[a] indicates the central atom

taken into account two interatomic distances labeled as H (Si–Si distance of 2.35 Å) and I (Si–Si distance of 3.84 Å).

Comparison of the results for all different properties presented in Table 3 allows us to conclude the following:

(a) The MBO's for the Fe–Si bonds in the FeSi clusters, as well as in the case of the Fe–Si diatomic molecule, are in essence of the *sp-sp* type.

(b) The charge transfer in the FeSi clusters takes place from the Si to the Fe atoms; this is contrary to what is found in the diatomic molecule. Comparison of the iron valence orbital population (VOP) in the diatomic molecule ($(sp)^{1.9}$, $d^{6.0}$) with the correspondent average value in the FeSi clusters ($(sp)^{1.6}$, $d^{7.0}$), (plus the fact that the Fe(d)–Si(sp) overlap is negligible) indicates that there is a bonding charge transfer from Si(sp) to Fe(sp), followed by an internal shift of electronic density to the Fe(d) orbitals. The experimental results for the polarity of the Fe–Si bond in FeSi bulk are controversial. XPS results of Sergughin et al. [3] indicate that the Si($2p$) levels in monosilicides are displaced to lower energies; this is interpreted to be the result of a reduction of the electronic density in silicon atoms. On the other hand, XPS reults of Egert and Panzner [1] show that the Si($2s$), Si($2p$), Fe($3p$), Fe($2p$) binding energies of the core levels decrease with respect to Si and Fe pure systems. They suggest the presence of a homopolar bonding character with a small charge transfer between iron and silicon atoms. A similar conclusion is reached from XPS results of Nemoshkalenko et al [2]. Our VOP results clearly indicate a transfer of electronic charge from the Si atoms to the Fe atoms, in spite of the fact that in the diatomic molecule the electronic drift is in the opposite direction. Nevertheless, one should keep in mind that the experimental results refer to bulk matter. Clearly our results are affected by the small number of atoms used to represent the Fe–Si bulk. Furthermore, one should consider that perhaps the charge separation obtained by a Mulliken population analysis may be deficient [28] and also that our basis set does not include polarization functions, such as $3d$ orbitals on silicon.

(c) The Fe–Si bond energies and bond orders involving the central Fe atom in Fe_7Si_7 (or central Si atom in Si_7Fe_7) are smaller than those of the peripheral Fe–Si bonds. This means that the Fe–Si bonds involving border atoms are tighter than those involving completely coordinated atoms.

(d) In the iron and FeSi clusters, the Fe–Fe bonds are mainly of *sp-sp* character; this is in agreement with both previous calculations [14], and also with experimental and theoretical results for homonuclear diatomic molecules of transition metals [29].

(e) The Fe(d) population in the Fe_{15} cluster ($d^{7.0}$) is quite similar to that obtained for the FeSi clusters; therefore, Fe d-orbital delocalization is not expected when one goes from pure iron to iron silicide. However, the Fe(sp) population in the FeSi clusters is greater than in Fe_{15} due to charge drift from the Si atoms.

(f) Comparison of the Fe–Fe and Si–Si diatomic energies in pure Fe_{15} and Si_{17}

clusters and in bimetallic Si_7Fe_7 and Fe_7Si_7 ones indicates that the Fe–Fe bond strength decreases from −0.021 to −0.041 a.u. for the central bonds and from −0.113 to −0.037 a.u. for the peripheral bonds. In addition, Si–Si bonds are weaker in the FeSi clusters than in the silicon cluster. In fact, the Si–Si diatomic energy diminished from −0.377 a.u. in Si_{17} to −0.024 a.u. in Si_7Fe_7 for the central bonds, and from −0.395 a.u. in Si_{17} to −0.019 a.u. in Si_7Fe_7 for the edge bonds. These bond strength changes can be accounted for by the increase of the Fe–Fe (2.48 Å to 2.75 Å) and Si–Si bond distances (2.35 Å to 2.78 Å) in going from pure clusters to Fe–Si clusters. The Fe–Fe and Si–Si bond depleting is compensated, therefore, by the formation of the Fe–Si bond. This effect is corroborated by the analysis of the calculated cohesive energy (CE) (total binding energy divided by the total number of atoms) for each cluster. In fact, for the Fe_{15} and Si_{17} clusters, the CEs are 4.1 eV (4.3 eV [30]) and 4.8 eV (4.7 eV [30]), respectively. They are very similar to the corresponding values of 4.0 eV and 4.2 eV for Fe_7Si_7 and Si_7Fe_7, respectively.

(g) Another interesting feature is found in connection with the calculated charge distribution in the Si_{17} cluster. The central Si atom is positively charged (+0.32 a.u.), its nearest 4 Si neighbors have an electronic charge of −0.32 a.u. per atom and the peripheral 12 Si atoms are electron deficient (+0.08 a.u. per atom). This alternate charge distribution has also been found in the Fe_{15} cluster suggesting that a cyclic charge distribution may exist in a real symmetric cluster. One possible explanation for these heterogeneous charge distributions arises from the difference in bond saturation between peripheric and central atoms. The less saturated atoms have the tendency to supply electrons to the most saturated ones. A similar effect was found in theoretical calculations with less symmetrical metallic clusters [14].

(h) The Fe–Si bonds in the FeSi clusters are stronger in magnitude than the Fe–Fe and Si–Si bonds. This is in agreement with experimental results reported by Goldschmidt [31], which established that the Si atoms are isolated and are bonded to the metal atoms only, and stands in contrast with the electron spectroscopy studies of Egert and Pazner [1] who concluded that the Si–Si interaction prevails in iron monosilicide.

(i) The DE terms and the total energy (−162.390 a.u.) for the Si_7Fe_7 cluster are larger in magnitude than the corresponding DE and total energy (−162.285 a.u.) in Fe_7Si_7 suggesting that the most stable system is formed by a central Si atom surrounded by Fe atoms as first neighbors. This energy difference would favour any structure in which Si atoms are placed within Fe atom cages. In other words, it would favour the migration of Si atoms placed on the surface of Fe bulk toward the interior of the Fe phase and, of course, it would not favour the migration of Fe atoms toward the interior of bulk Si. This conclusion correlates well with the experimental work of Lau et al. [32], who indicate that the Si atoms were the moving species during the growth of FeSi phase from thin layers of Fe deposited onto a single Si crystal.

(j) Comparison of MBO's and DE's for Fe_7Si_7 and Si_7Fe_7 indicates that no

correlation exists between them (FeSi has smaller DE's than SiFe, while the MBO's in FeSi are larger than in SiFe). The difference between these two bonding parameters lies in the fact that the MBO's consider only the terms that involve interatomic overlapping, while, in the DE, coulombic terms are also included. These results suggest that the coulombic interactions have an important bearing on the nature of the Fe–Si bond.

A more detailed analysis of FeSi diatomic energies, such as was done in [17], can be utilized to explain the role of Fe-*d* orbitals in the Fe–Si bond. For this purpose, let us further partition the electronic diatomic energy into resonance energy (RE), attraction energy between electrons and nuclei (AE), exchange energy of electrons (EE), and repulsion energy of electrons (REE). Each energy term is decomposed into *s-s*, *p-p*, *d-d*, *s-p*, *s-d*, and *p-d* components as shown in Table 4 for the Fe*–Si(*A*) diatomic energy (−0.132 a.u., see Table 3). The *s-s* term includes the electron attraction between the Fe(*s*) electron density with the Si nucleus, and between Si(*s*) electron density with the Fe nucleus. The *p-p* and *d-d* terms are treated similarly. Therefore, the nuclear-attractions are not included in the *s-p*, *s-d* and *d-p* terms. Although a complete partitioning of energy has been performed, it is difficult to discern, for instance, the specific contribution to the DE coming only from *d* orbitals. For this reason, we assume the following criterion for calculating the total energy contribution of a particular orbital, TE(*j*) ($j = s, p, d$), to the diatomic energy. The criterion is based on the relative weight given by the orbital occupation numbers:

$$\mathrm{TE}(s) = \mathrm{TE}_{s\text{-}s} + \alpha_{s\text{-}p}\,\mathrm{TE}_{s\text{-}p} + \alpha_{s\text{-}d}\,\mathrm{TE}_{s\text{-}d}$$

$$\mathrm{TE}(p) = \mathrm{TE}_{p\text{-}p} + \alpha_{p\text{-}s}\,\mathrm{TE}_{s\text{-}p} + \alpha_{p\text{-}d}\,\mathrm{TE}_{p\text{-}d}$$

$$\mathrm{TE}(d) = \mathrm{TE}_{d\text{-}d} + \alpha_{d\text{-}s}\,\mathrm{TE}_{s\text{-}d} + \alpha_{d\text{-}p}\,\mathrm{TE}_{p\text{-}d}$$

where, $\alpha_{j\text{-}k} = n_j/(n_j + n_k)$ (n_j is the *j*-type orbital population). Because the term $\mathrm{TE}_{s\text{-}p}$ is associated with Fe(*s*)–Si(*p*) and Si(*s*)–Fe(*p*) interactions, the n_s and n_p populations utilized in the calculation of the $\alpha_{s\text{-}p}$ and $\alpha_{p\text{-}s}$ weighting factors have to include the *s* and *p* population of both iron and silicon atoms. In the case of $\alpha_{s\text{-}d}$, $\alpha_{d\text{-}s}$, $\alpha_{p\text{-}d}$ and $\alpha_{d\text{-}p}$, the n_s and n_p values only consider the *s* and *p* population over the silicon atom.

With this in mind, the values of TE(*s*) = −1.9873 a.u., TE(*p*) = −3.0732 a.u. and TE(*d*) = −1.8239 a.u. were obtained from Tables 3 and 4, and the iron and silicon atoms *s*-population (n_s(Fe) = 0.38 and n_s(Si) = 1.30). These results indicate a noticeable energetic participation of the *d* orbitals in the Fe–Si bond resulting from the strong attractive stabilizing interaction between the *d* orbitals and the Si nucleus as shown in the fourth column of Table 4.

Iterative extended Hückel calculations for other metal silicides by Bisi et al. [33] reveal that the *d* orbitals participate directly in the Fe–Si bond. Nevertheless, in our calculations the direct participation of the *d* orbitals in the Fe–Si bond (covalent bond) is indeed negligible. This can be explained by observing the small overlap values betwen iron *d* orbitals and silicon *s-p* orbitals. The optimized single zeta *d*-orbital exponent (3.72669 (a.u.)$^{-1}$) given in [33] is employed

Table 4. Partitioning of Fe^a–Si(A) diatomic energy (shown in Table 3 for the Fe_7Si_7 cluster) and FeSi (diatomic molecule) diatomic energy (values in parentheses). AE (attraction energy between electrons and nuclei), EE (exchange energy of electrons), RE (resonance energy), REE (repulsion electron-electron), and TE (total energy interaction for j-k orbitals, where j or k are s, p, d orbitals). Energies are in a.u.

Energy type	Orbitals						Total
	s-s	*p-p*	*d-d*	*s-p*	*s-d*	*p-d*	
AE	−2.4100	−4.4507	−5.7816	—	—	—	−12.6423
	(−3.4225)	(−4.5719)	(−5.0509)	—	—	—	(−13.0454)
EE	−0.0027	−0.0091	—	−0.0140	−0.0001	−0.0008	−0.0267
	(−0.0099)	(−0.0466)	—	(−0.0870)	(−0.0000)	(−0.0026)	(−0.1461)
RE	−0.0540	−0.0790	—	−0.1822	−0.0006	−0.0027	−0.3185
	(−0.1041)	(−0.1218)	—	(−0.4517)	(−0.0003)	(−0.0051)	(−0.6829)
REE	0.1004	0.4917	—	0.4622	1.8743	3.1746	6.1031
	(0.3449)	(0.3562)	—	(0.7710)	(1.9389)	(3.0657)	(6.4768)
TE	−2.3663	−4.4507	−5.7816	0.2659	1.8736	3.1711	−0.1318[a]
	(−3.1916)	(−4.3841)	(−5.0509)	(0.2323)	(1.9386)	(3.0581)	(−0.5216)[a]

[a] The nuclear repulsion energy for Fe^a–Si(A) (6.7526 a.u.) or for the diatomic molecule (6.8759 a.u.) has been added

in these calculations. It produces for the Fe–Si diatomic molecule the values of 0.025, 0.040, 0.402, 0.565 and 0.284 for s-d_{z^2}, p_z-d_{z^2}, s-s, s-p_z and p_z-p_z overlaps, respectively. A test, using the lowest Clementi–Roetti's exponent (2.61836 (a.u.)$^{-1}$) for double zeta functions [34], was carried out and the results showed a fair improvement for the s-d_{z^2} and p-d_{z^2} overlaps (0.075 and 0.098, respectively). However, the sp-d bond orders are still considerably smaller than the sp-sp ones. Similar results have also been found by MINDO/SR calculations on FeCO systems carried out by Blyholder and Lawless [35] using double zeta functions for Fe(d) orbitals. Discussions about d-orbital participation in transition metal compounds have been reported previously [16, 18]. In a review of Ni–H calculations [18] performed at different levels of sophistication, it was pointed out that several authors are of the opinion that d-orbital participation in the Ni–H bond is certainly small. On the other hand, other researchers support the idea that d orbitals participate directly in this bond. In order to settle this controversial issue a thorough analysis using extended basis sets as well as CI methods should perhaps be carried out. It is necessary to improve the representations of s, p and d orbitals, and also to take into account the interaction of several excited configurations that contain an electronic densities distribution which favor the direct d orbital participation in the Fe–Si bond.

One important question is why the diatomic molecule has d^6 occupation while the cluster has d^7. In Table 4, the partitioning of the diatomic energy (see above) for the Fe_7Si_7 cluster and the FeSi diatomic molecule is compared (see values in parentheses for the diatomic molecule). As expected, the d-d attractive term is smaller in the diatomic molecule than in the cluster. The opposite is true for the s-s and p-p terms. In addition, there is a considerable increase in the resonance energy terms of the diatomic molecule. This is reflected in the fact that the Fe–Si bond is stronger in the diatomic molecule (bond order of 2.03) than in the cluster (0.93). Because the iron atom in the cluster is surrounded by seven silicon atoms, and because the attraction between d electrons and the silicon nuclei is an important factor affecting the system's stability, a redistribution of the electron density on the d orbitals toward the positions of the silicon atoms is favored. Thus, we have the following d-orbital occupations: d_{z^2} ($1.33e^-$), d_{xz}($1.24e^-$), d_{yz}($1.67e^-$), $d_{x^2-y^2}$($1.23e^-$) and d_{xy}($1.53e^-$). This type of electronic redistribution cannot occur in the case of the FeSi diatomic molecule since much of the d-orbital density is far from the Si nucleus and it is more favorable to transfer d electrons to s and p orbitals by the mechanism of hybridization, increasing the electronic density in the internuclear zone.

3.4. Density of states

The total densities of states (DOS) for the Fe_7Si_7, Si_7Fe_7 and Fe_{15} clusters calculated using the method mentioned in Sect. 2 are presented in Fig. 4. Comparison of Fe_7Si_7 and Si_7Fe_7 DOS indicates that they are quite similar except for the presence of some small sp-peaks in Si_7Fe_7 which are displaced to lower energies. The displacement at lower energies is larger in Si_7Fe_7 than in

Fe_7Si_7 which correlates well with the DE values presented in Table 3, and with the fact that the *sp-sp* MBO's are larger for Si_7Fe_7 than for Fe_7Si_7. However, there is a noticeable DOS difference in the position of the peaks between the iron and iron silicide clulsters. For the purpose of clarifying the meaning of these peaks, the DOS of Fe_7Si_7, Si_7Fe_7, Fe_{15} and Si_{17} for *d* and for *sp* electrons are presented in Figs. 5 and 6, respectively. The *d*-DOS suggest that the *d* orbitals are localized in both the iron and the iron silicide clusters. In fact, a check on the *d* molecular orbitals confirms that most of the energy levels are associated with a few atoms and in many cases with a single atom with very small *spd* hybridization. The *d* band width of iron, measured as the width of the peak at half its maximum in Fig. 5, equals 3.98 eV. This is comparable with the 5.0 eV

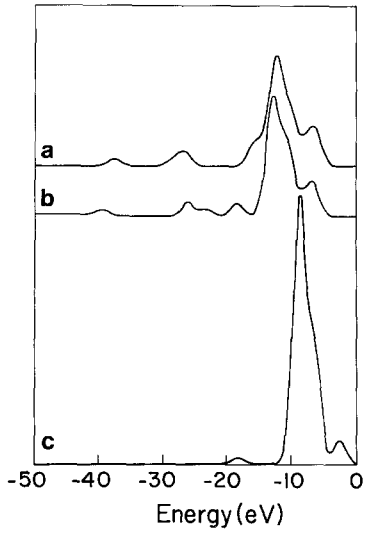

4

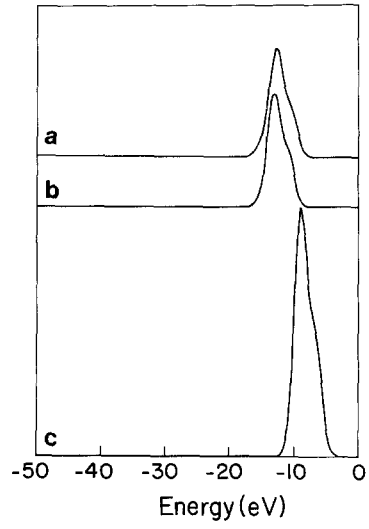

5

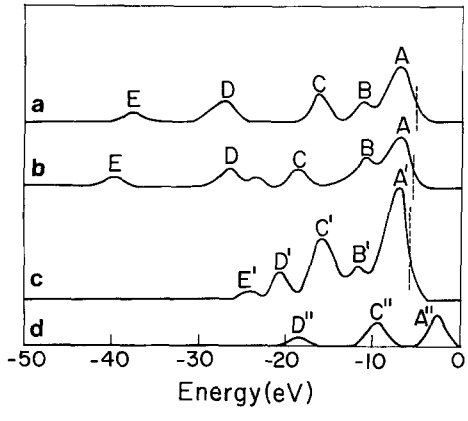

6

Fig. 4. Total density of state. **a** Fe_7Si_7; **b** Si_7Fe_7; **c** Fe_{15}

Fig. 5. Density of state for *d* electrons. **a** Fe_7Si_7; **b** Si_7Fe_7; **c** Fe_{15}

Fig. 6. Density of state for *sp* electrons. **a** Fe_7Si_7; **b** Si_7Fe_7; **c** Si_{17}; **d** Fe_{15}

value obtained in band theory calculations for Fe bulk [36] and with the 4.4 value from MINDO/SR calculations on a Fe_{12} cluster [14].

A significant change in the position of the *d* band is observed in iron with respect to iron silicide. The FeSi *d* band moves toward lower energy (more negative) with respect to the Fermi level. This result is qualitatively in agreement with experimental X-ray photoemission valence-band spectra [1]. In fact, experimental results in which the valence band of clean iron has been subtracted from those of iron silicides clearly show that the binding energy of *d* electrons increases with the silicon content so that a portion of the *d*-intensity is displaced from a region close to the Fermi energy to regions of lower energy. The explanation of the energy-lowering of the *d* orbitals (which do not overlap with the atomic orbitals of neighboring atoms) is given by the electrostatic nuclear-electron interaction. As we pointed out above, the DE analysis of the Fe–Si bond (in the FeSi cluster) reveals a considerable attractive interaction between the *d* electrons and the Si nucleus; this is enhanced by the facts that Si atoms are positively charged and are located at distances less than the nearest neighbors distance in the iron cluster.

For bimetallic and metallic clusters MINDO/SR has the tendency to produce a *sp*-band which is too broad, and a *sp*-peak which is closer to the Fermi level than the *d*-band [14, 16, 18]. These effects have been also observed in *ab initio* [37] and INDO semiempirical calculations [38]. An explanation of this broadening, in the Fe_{15} cluster is obtained by a careful study of the origin of each *sp*-peak. The hump closer to the Fermi level does not have any contribution coming from the central (completely coordinated) atom; therefore, it is a direct consequence of the unsaturated Fe atoms at the border of the small iron cluster model used in the present work.

In what follows, we advance an explanation for the origin of the Fe_7Si_7 (or Si_7Fe_7) peaks, shown in Fig. 6; this is done in terms of the Fe_{15} and Si_{17} DOS's of the isolated systems. In Fig. 6a for Fe_7Si_7 (or Fig. 6b for Si_7Fe_7), in the region of smallest binding energy, we observe three peaks marked as *A*, *B* and *C*. Comparison with Fig. 6c for Si_{17} clearly suggests that peaks *A* and *B* are essentially the silicon peaks *A'* and *B'* which, in fact, are slightly stabilized by a small Si(3*p*)–Fe(4*s*, 4*p*) interaction which is 70% localized on the Si atoms. A check for the origins of the iron peaks, shown on Fig. 6d, reveals that the *A''* peak has a (4*s*, 4*p*) nature; hence, they correlate with the *A* and *B* peaks of iron silicide. Peak *C* for Fe_7Si_7, in Fig. 6a, is associated mainly with the silicon peak labeled *C'* for Si_{17} and it is slightly stabilized by a small Si(3*s*)–Fe(4*p*) interaction since it is 65% localized on Si(3*p*) with a very small 4*p*-3*d* hybridization. Peak *C* shown in Fig. 6b has a larger participation of Fe(4*p*) (about 42%) which makes it more spread out for Si_7Fe_7 than for Fe_7Si_7. In accord with the nature of the *C*, *C'* and *C''* peaks, the *C* peaks of Figs. 6a–b stem mainly from *C'* and partly from *C''* (Fe(4*p*)).

It should be mentioned that our calculated *A*, *B* and *C* peaks in Fig. 6a are located at about 2.5, 5.5 and 11.0 eV with respect to the Fermi level which is indicated by a vertical dashed line. The BIS experimental results of Oh et al. [4] reported three peaks (labeled by *B*, *C* and *D* in Fig. 1 of [4]) at about 2.5,

5.0–5.5 and 9.0–10.5 eV assigned to non-bonding Fe(3*d*), Si(3*p*) and Si(3*s*) states, respectively. This close agreement between the position of experimental and theoretical DOS bands suggests that the peak *B* given by Lo et al. at 2.5 eV may be a consequence of overlap between the *sp*-band and the *d*-band. The other two peaks are in agreement with the present assignment although our calculations show that they are not pure Si(3*p*) and Si(3*s*) as suggested by Oh et al. [4] and Egert and Panzner [1], but a mixture of these with the Fe(4*s*) and Fe(4*p*) orbitals.

Peaks *D* and *E* shown in Fig. 6a for Fe_7Si_7 are associated with a strong bonding interaction among the Si(3*s*) and the Fe(4*s*) and Fe(4*p*) orbitals. These two peaks located at about 21.5 and 32.5 eV with respect to the Fermi level seem to be very strongly shifted in energy. As was noted above, the MINDO/SR has the tendency to produce a *sp*-band which is too wide. However, this result is not unusual because calculations on the *ab initio* MgO diatomic molecule carried out in our group with the Monster–Gauss program [39] showed a shift of 22.0 eV between the HOMO and the most stable occupied valence orbital. On the other hand, it is known that peaks below 10 eV are not clearly observed in the experimental UPS spectrum, probably due to a secondary electron effect which masks the primary electron transitions. An analysis of the molecular orbitals contributing to the *D'* and *E'* peaks showed that they are essentially Si(3*s*), whereas *D''* peak is formed of Fe(4*s*) and Fe(4*p*) orbitals. These results clearly suggest that the *D* and *E* peaks in iron silicide come from the *E'* and *D'* peaks in silicon and the *D''* peak in iron. The origin of *E* and *D* peaks in Si_7Fe_7 (Fig. 6b) may be similarly explained.

Finally, let us mention that our present DOS and charge transfer results for Fe_7Si_7 and Si_7Fe_7 clusters coincide with unpublished results for $Fe_{12}Si_{12}$ and $Si_{12}Fe_{12}$ clusters used to study chemisorption of oxygen on a FeSi (100) surface [40].

Acknowledgments. The authors would like to express their gratitude to Drs. Claudio Mendoza, Juan Rivero, Walter Cunto and Miguel Luna of the IBM Venezuela Scientific Center for assistance with computer programs. A computer time grant on the 3081 computer at IBM Venezuela is gratefully acknowledged. L.R. would like to thank the "Consejo Nacional de Investigaciones Científicas y Tecnológicas" CONICIT, for financial support.

References

1. Egert B, Panzner G (1984) Phys Rev B: Solid State 29:2091
2. Nemoshkalenko VV, Zakharov AI, Aleshin VG, Matveev YA (1977) Theor Exp Chem 13:529
3. Sergushin NP, Shabanova IN, Kolobova KM, Trapeznikov VA, Nefedov VI (1973) Fiz Metal Metalloved 35:947
4. Oh SJ, Allen JW, Lawrence JM (1987) Phys Rev B: Solid State 35:2267
5. Kohgi M, Ishikawa Y (1981) Solid State Comm 37:833
6. Kakizaki A, Sugawara H, Nagakura I, Ishikawa Y, Komatsubara T, Ishii T (1982) J Phys Soc Japan 51:2597
7. (a) Zhu Q, Iwasaki H, Williams ED, Park RL (1986) J Appl Phys 60:2692; (b) Ballesteros A, Rojas CE, Castro GR (1987) In: Castro GR, Cardona M (eds) Lectures in Surface Science. Springer, Berlin Heildelberg New York

8. (a) Wertheim GK, Jaccarino V, Wernick JH, Seitchik JA, Williams HJ, Sherwood RC (1965) Phys Letters 18:89; (b) Evangelou SN, Edwards DM (1983) J Phys C: Solid State Phys 16:2121; (c) Klimker H, Perz JM, Svechkarev IV, Dolgopolov DG (1986) J Mag Mag Materials 62:339; (d) Kvardakov VV, Podurets KM, Chistyakov RR, Shilshtein SS, Elyutin NO, Kulidzhanov FG, Bradler J, Kadeckova S (1987) Sov Phys Sol State 29:228; (e) Shirane G, Fischer JE, Endoh Y, Tajima K (1987) Phys Rev Letters 59:351
9. (a) Nikitin EN, Tarasov VI (1971) Sov Phys Cryst 16:305; (b) Panfilov AS (1985) Sov Phys Semicond 19:1159
10. Rodríguez LJ, Ruette F, Ludeña EV, Castro GR, Henández AJ (1987) In: Castro GR, Cardona M (eds) Lectures in Surface Science. Springer, Berlin Heidelberg New York
11. Blyholder G, Head J, Ruette F (1982) Theor Chim Acta 60:429
12. Bingham RC, Dewar MJS, Lo DH (1975) J Am Chem Soc 97:1285
13. Head J, Blyholder G, Ruette F (1982) J Comp Phys 45:255
14. Blyholder G, Head J, Ruette F (1983) Surface Sci 131:403; Ruette F, Blyholder G, Head J (1984) Surface Sci 137:491
15. Ruette F, Blyholder G, Head J (1984) J Chem Phys 80:2042
16. Ruette F, Hernández AJ, Ludeña EV (1985) Surface Sci 151:103
17. Ruette F, Ludeña EV, Hernández AJ (1986) Int J Quantum Chem XXIX:1351
18. Ruette F, Ludeña EV, Hernández AJ, Castro GR (1986) Surface Sci 167:393
19. Ruette G, Blyholder G (1988) Theor Chim Acta 74:137
20. Rosen B (1970) Spectroscopic data relative to diatomic molecules. Pergamon Press, Oxford New York
21. Edwards AH, Fowler WB (1985) J Phys Chem Solids 46:841; ibid. (1982) Phys Rev B26:6649; Cuthbertson AF, Glidewell C (1981) Inorganic Chim Acta 49:91
22. Gingerich KA (1980) In: Kadis E (ed) Current topics in materials science, vol 6, Chap 5. Elsevier/North-Holland, Amsterdam New York, p 345
23. Simonetta M, Gavezzotti A (1980) In: Lowdin P (ed) Advances in quantum chemistry, vol 12. Academic Press, New York, p 103
24. Pople, J. A. Beveridge, D. L. (1970) Approximate molecular orbital theory. Pergamon Press, New York
25. Moffat JB, Tang KF (1975) J Phys Chem 79:654
26. Hansen M (1958) Constitution of binary alloys. McGraw-Hill, New York
27. Pauling L, Soldate AM (1948) Acta Cryst 1:212
28. (a) Fliszár S (1983) Charge distributions and chemical effects. Springer, Berlin Heidelberg New York, p 27; (b) Slee TS (1986) J Am Chem Soc 108:7541
29. (a) Shim I, Gingerich KA (1982) J Chem Phys 77:2490; (b) Morse MD, Hansen GP, Landridge-Smith PRR, Zheng LS, Geusic ME, Michalopoulos DL, Smalley RE (1984) J Chem Phys 80:5400
30. (a) Skinner A, Pilcher B (1963) Quart Rev 17:264; (b) Kittel C (1971) Introduction of solid state physics. Wiley, New York, p 96
31. Goldschmidt HJ (1967) Interstitial alloys. Butterworths, London
32. Lau SS, Feng JSY, Olowolafe JO, Nicolet MA (1975) Thin Solid Films 25:415
33. (a) Bisi O, Calandra C (1981) J Phys C: Solid State Phys 14:5479; (b) Abbati I, Braicovich L, De Michelis B, Bisi O, Rovetta R (1981) Solid State Comm 37:119
34. Clementi E, Roetti C (1974) Atomic data and nuclear tables. Academic Press, New York London
35. (a) Blyholder G, Lawless M (1987) Prog Surf Science 26:181; (b) Blyholder G, Lawless M (1989) J Am Chem Soc 111:1275
36. Tavil RA, Callaway J (1973) Phys Rev B 7:4242
37. (a) Demuynck RC, Rohmer MM, Strich A, Veillard A (1981) J Chem Phys 75:3443; (b) Basch H, Newton MD, Moskowitz JW (1980) J Chem Phys 73:4492
38. (a) Rodríguez JA, Campbell CT (1987) J Phys Chem 91:2161; (b) Rodríguez JA, Campbell CT (1987) Surface Sci 183:449
39. MONSTERGAUSS (1981) Peterson MR, Poirier RA, Department of Chemistry, University of Toronto, Canada
40. Rodríguez LJ, Ruette F, Ludeña EV, Castro GR, Hernández A (1987) In: Castro GR, Cardona M (eds) Lectures in Surface Science. Springer, Berlin Heidelberg New York, p 132